



Search for Majorana neutrinos

Itaru Shimizu*

Research Center for Neutrino Science, Tohoku University, Sendai 980-8578, Japan

*E-mail: shimizu@awa.tohoku.ac.jp

Received February 28, 2023; Accepted March 14, 2023; Published March 15, 2023

.....
Whether there exist elementary particles having Majorana nature is a fundamental open question that has persisted since the 1930s. The only practical experiments to test the Majorana nature of neutrinos is the search for neutrinoless double-beta decay, which has been a major challenge for nuclear and particle physicists. In the 2000s, a number of experiments using advanced technologies were planned, some of which have already achieved significant improvements in the search sensitivity. In this article, the current status of the neutrinoless double-beta decay searches is summarized, reviewing the progress of KamLAND-Zen, which recorded the world's best sensitivity in the effective Majorana neutrino mass limit.
.....

Subject Index C43, D02

1. Introduction

Neutrinos are elementary particles that have no electric and color charges, and interact weakly with other particles. According to standard cosmology, neutrinos are the most abundant fermions in our universe. Understanding the properties of neutrinos is of great importance for particle physics and cosmology; however, their experimental study is not easy because of their rare interactions with matter. After long-standing efforts, observations of neutrino oscillation have revealed that neutrinos have tiny masses, the first discovery of physics beyond the Standard Model (SM). Since neutrino masses are much smaller than those of other fermions, the origin of neutrino masses must be something special. An uncharged neutrino particle could be its own antiparticle, the so-called Majorana neutrino, proposed by Ettore Majorana in 1937. This hypothesis is important to build a theoretical mechanism for tiny neutrino masses: right-handed heavy neutrinos with Majorana masses on the grand unified theory (GUT) scale naturally lead to light neutrino masses (see-saw mechanism); however, so far there is no experimental evidence to support the theory. In addition, the CP -violating decay of heavy neutrinos in the early universe can also explain the matter dominance in the universe (leptogenesis). The Majorana neutrino is a key piece of particle physics and cosmology, and the determination of its relevant parameters, the masses and CP phases of the Majorana neutrino, is of critical importance. In this article, I review the recent status of the experimental search for the Majorana neutrino.

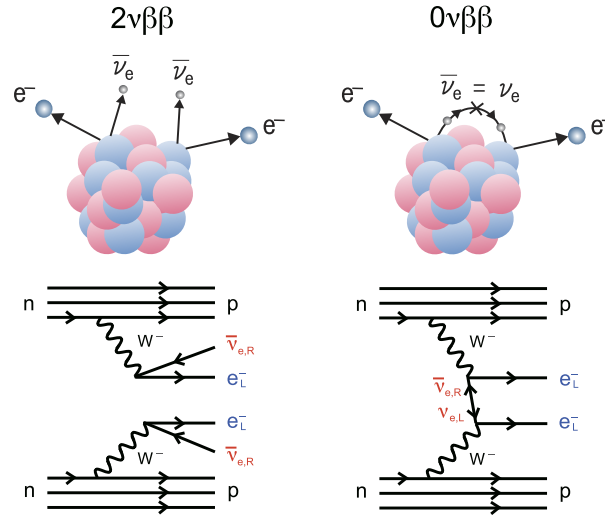


Fig. 1. Decay scheme and Feynman diagrams for $2\nu\beta\beta$ (left) and $0\nu\beta\beta$ (right).

2. Majorana neutrino

Neutrinos were first introduced by W. Pauli in 1930 to reconcile an anomaly in the conservation of energy and spin in nuclear beta decay. Experimental observation of neutrinos has been difficult for decades because they interact with other particles only through weak interactions. Double-beta ($\beta\beta$) decay, equivalent to two simultaneous β decays, was first proposed by M. Goeppert-Mayer in 1935 [1], soon after the quantitative theory of β -ray emission by E. Fermi. Double-beta decay is observable if one decay is suppressed by energy levels or spin states, but two simultaneous decays are not. In 1937, E. Majorana suggested the possibility of an uncharged neutrino particle being its own antiparticle. Based on this hypothesis, in 1939, W. H. Furry proposed the idea of double-beta decay with no neutrino emission at all, now called neutrinoless double-beta decay ($0\nu\beta\beta$) [2],

$$(A, Z) \rightarrow (A, Z+2) + 2e^-, \quad (1)$$

emitting only two electrons, explicitly violating the lepton number by two (Fig. 1). $0\nu\beta\beta$ decay can be realized when two electron antineutrinos annihilate inside a nucleus, while such a process is forbidden in the SM, and can be an excellent probe of the Majorana neutrino.

On the other hand, the SM-allowed second-order nuclear decay is two-neutrino double-beta decay ($2\nu\beta\beta$),

$$(A, Z) \rightarrow (A, Z+2) + 2e^- + 2\bar{\nu}_e, \quad (2)$$

emitting two electrons and two electron antineutrinos (Fig. 1). Since $0\nu\beta\beta$ decays do not emit antineutrinos and have a monoenergetic energy peak at the Q -value, they can be experimentally distinguished from $2\nu\beta\beta$ by observing the total energy of the two electrons. The first experimental search was conducted by E. L. Fireman in 1948 using Geiger counters and 25 g of enriched ^{124}Sn [3]. Subsequent experiments used a variety of particle detectors, such as Geiger, proportional, and scintillation counters. The initial $0\nu\beta\beta$ search experiments often found false positive signals, later disproved by other experiments. After the discovery of maximal parity violation in weak interactions in 1957, the predicted decay rate for $0\nu\beta\beta$ was more highly suppressed than that for $2\nu\beta\beta$, so the search for Majorana neutrinos via $0\nu\beta\beta$ was recognized for a time to be a challenging task.

The discovery of the neutrino oscillation is a hopeful sign for the $0\nu\beta\beta$ search, as $0\nu\beta\beta$ may be mediated by an exchange of light Majorana neutrinos, as shown in Fig. 1. In the case of a massless Majorana neutrino, right-handed $\bar{\nu}_e$ emitted from a neutron has the wrong helicity ($h = +1$) for absorption on another neutron; however, neutrinos should have finite masses to cause neutrino oscillation, so it can undergo a helicity flip ($h = -1$) with a probability depending on the masses. In the model of light Majorana neutrino exchange, the $0\nu\beta\beta$ decay rate (inverse half-life) is

$$(T_{1/2}^{0\nu})^{-1} = G_{0\nu} |M_{0\nu}|^2 \langle m_{\beta\beta} \rangle^2, \quad (3)$$

where $G_{0\nu}$ is the phase-space factor, $M_{0\nu}$ the nuclear matrix element (NME), and $\langle m_{\beta\beta} \rangle$ the effective Majorana neutrino mass. $G_{0\nu}$ can be accurately calculated based on the wave function of the electron in the Coulomb field of the nucleus. On the other hand, since the evaluation of the NME requires dealing with complex nuclear structure, so the theoretical estimate of NME strongly depends on the many-body approach used in the calculation. Considering the dependence on the calculation method, the value of $|M_{0\nu}|$ will have an uncertainty of a factor of 2–3.

As indicated in Eq. (3), the decay rate increases with the square of the effective Majorana neutrino mass

$$\langle m_{\beta\beta} \rangle = \left| \sum_i U_{ei}^2 m_{\nu_i} \right|, \quad (4)$$

where U_{ei} is the 3×3 unitary neutrino mixing matrix, and m_{ν_i} are the masses of three neutrinos (ν_1, ν_2, ν_3). It is important to note that this sum includes complex CP phases in U_{ei} (one Dirac and two Majorana CP phases), so cancellations can occur. Measurements of the neutrino oscillation have determined the three mixing angles ($\theta_{12}, \theta_{23}, \theta_{13}$) and two square mass differences ($0 < \Delta m_{21}^2 \ll |\Delta m_{32}^2|$, where $\Delta m_{ij}^2 = m_{\nu_i}^2 - m_{\nu_j}^2$), while the ordering of three neutrino masses (sign of Δm_{32}^2) is still uncertain. Thus, there are two possibilities for the mass ordering in the three neutrinos, normal ordering (NO) with one heavier neutrino relative to the other two ($m_{\nu_1} < m_{\nu_2} \ll m_{\nu_3}$), or inverted ordering (IO) with two heavier neutrinos ($m_{\nu_3} \ll m_{\nu_1} < m_{\nu_2}$). If the lightest mass is zero, the predicted range of $\langle m_{\beta\beta} \rangle$ based on the best-fitting values of neutrino oscillation parameters [4] is 1–4 meV and 19–48 meV for NO and IO (Fig. 2), respectively, where the uncertainty in $\langle m_{\beta\beta} \rangle$ is due to the Majorana CP phases. Thus, the experimental constraints on $\langle m_{\beta\beta} \rangle$ provide information on the absolute neutrino mass scale and ordering.

In general, order 1 ton of $\beta\beta$ isotopes is required to obtain a sensitivity of $\langle m_{\beta\beta} \rangle$ down to 10–20 meV. The sensitivity that an experiment can reach depends on the background level achieved in the experiment, and the NME and phase-space factor of the isotope selected. Most of the near-future experiments aim at probing the IO region. To probe down to a few meV, corresponding to the NO region, experiments would need to increase their exposures by about two orders of magnitude using order 100 ton of $\beta\beta$ isotopes (Fig. 2).

The absolute neutrino mass can also be probed by other approaches that do not assume the Majorana nature of the neutrino. Precise measurements of the electron energy spectrum in β decay are sensitive to the effective neutrino mass:

$$\langle m_\beta \rangle = \sqrt{\sum_i |U_{ei}|^2 m_{\nu_i}^2}. \quad (5)$$

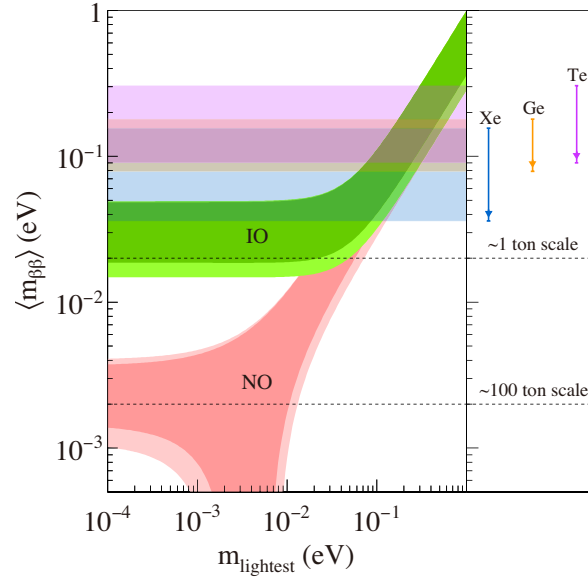


Fig. 2. Effective Majorana neutrino mass $\langle m_{\beta\beta} \rangle$ as a function of the lightest neutrino mass m_{lightest} . The dark shaded regions are predictions based on the best-fitting values of neutrino oscillation parameters for the normal mass ordering (NO) and the inverted mass ordering (IO), and the light shaded regions indicate the 3σ ranges calculated from oscillation parameter uncertainties [4,39]. The horizontal bands indicate 90% C.L. upper limits on $\langle m_{\beta\beta} \rangle$ with ^{136}Xe from KamLAND-Zen [22], ^{76}Ge [7], and ^{130}Te [9]. The horizontal dashed lines indicate the required mass scale of the $\beta\beta$ source to achieve deep exploration for each of the IO and NO regions.

The KATRIN experiment using tritium β decay reported the latest result, $\langle m_{\beta} \rangle < 0.8 \text{ eV}$ at the 90% confidence level (C.L.) [5]. In the future, KATRIN aims to reach a sensitivity of 0.2 eV [5], which covers the predicted $\langle m_{\beta} \rangle$ of IO. Furthermore, since massive neutrinos strongly influence the evolution of the large-scale structure of the universe, cosmological observations can place very strong constraints on the sum of the three neutrino masses:

$$\Sigma m_{\nu} = \sum_i m_{\nu_i}. \quad (6)$$

The Planck Collaboration reported a stringent upper limit of $\Sigma m_{\nu} < 0.12 \text{ eV}$ at 95% C.L. [6]. A positive value of Σm_{ν} from future observations would provide another milestone. If a positive $0\nu\beta\beta$ signal is found at the rate expected from other observations, it could prove the scenario of the light Majorana neutrino exchange. Even if it is negative, the contradiction with other observations would disprove the standard scenario, and could have a significant impact on particle physics and cosmology.

3. $0\nu\beta\beta$ search experiments

The basic idea of the $0\nu\beta\beta$ search is to observe two emitted electrons and find a monoenergetic peak in the energy spectrum of their sum. In order to achieve high sensitivity, various ideas were considered, utilizing new detector technologies and low-background techniques developed in neutrino observations, $\beta\beta$ decay, and dark matter searches.

The main background sources are $2\nu\beta\beta$, environmental radioactivities such as ^{238}U , ^{232}Th , and cosmogenic isotopes produced by muon spallation. The background of solar neutrinos should be taken into account if the target isotope concentration is small. The main features for significant background reduction are as follows:

- (1) Target nucleus increase per volume (isotope enrichment)
- (2) Good energy resolution (narrow energy window for $0\nu\beta\beta$ signal)
- (3) Thick shielding for external radiation (underground detector with active shield)
- (4) Particle identification (multisite energy deposits in γ background)
- (5) Sequential decay tagging (background rejection with space and time correlation)
- (6) Daughter nucleus tagging ($0\nu\beta\beta$ signal identification)

The statuses of the leading $0\nu\beta\beta$ experiments in the world are introduced below.

- GERDA

In this experiment, a semiconductor detector technique using enriched ^{76}Ge was developed. The detector consists of 44 kg of high-purity germanium (HPGe) and is deployed into a 64 m^3 cryostat containing ultra-pure liquid argon (LAr). It has a good energy resolution (FWHM) of 2.9 keV at the Q -value (2039 keV). The final GERDA result in 2020 provides a limit of $\langle m_{\beta\beta} \rangle < 79\text{--}180\text{ meV}$ at 90% C.L. [7]. A future 1 ton detector in the LEGEND experiment will aim for a sensitivity down to 9–19 meV [8].

- CUORE

The detector consists of 988 ultra-cold TeO_2 bolometers with natural tellurium for a total mass of 742 kg (206 kg of ^{130}Te). The NTD thermistor converts the thermal pulse into a resistance variation, realizing an FWHM energy resolution of 7.8 keV at the Q -value (2528 keV). The CUORE result in 2022 provides a limit of $\langle m_{\beta\beta} \rangle < 90\text{--}305\text{ meV}$ at 90% C.L. [9]. The CUPID experiment can use the same cryogenic infrastructure as CUORE for scintillating bolometers, replacing TeO_2 with Li_2MoO_4 enriched in the isotope of ^{100}Mo , and will aim for a sensitivity down to 10–17 meV [10].

- EXO

In this experiment, a liquid xenon time projection chamber (TPC), containing $\sim 175\text{ kg}$ of xenon enriched to 80.6% in ^{136}Xe (EXO-200) was developed. The liquid xenon (LXe) TPC is capable of simultaneously reading ionization and scintillation. The event position is obtained from the time delay between the prompt light and the delayed charge signals, and also multisite energy deposits can be identified. The final EXO-200 result provides a limit of $\langle m_{\beta\beta} \rangle < 94\text{--}286\text{ meV}$ at 90% C.L. [11]. Cosmogenically produced ^{137}Xe was a problematic background. Future plans to use 5 tons of enriched xenon in the nEXO experiment aim to have a sensitivity down to 6–18 meV, assuming a deeper experimental location at SNOLAB [12]. The possibility of tagging Ba daughters is also being explored.

- KamLAND-Zen

KamLAND has developed a xenon-loaded liquid scintillator detector (KamLAND-Zen), which has great advantages in the scalability of the $\beta\beta$ isotope amount. Details of the detector design and results are described in the next section.

There are a number of $\beta\beta$ experimental projects utilizing new detector technologies and low-background techniques, which are summarized in Ref. [13]. Calorimeter experiments, i.e., where the $\beta\beta$ source and detector are the same, are semiconductors (GERDA, MAJORANA, LEGEND), bolometers (CUORE, CUPID, AMoRE), liquid TPC (EXO), loaded liquid scintillator (KamLAND-Zen, SNO+, ZICOS), inorganic scintillator (CANDLES), and high-pressure gas TPC (NEXT, AXEL, PandaX-III) experiments. On the other hand, external source experiments (NEMO) use thin sources that allow electrons to escape without significant energy

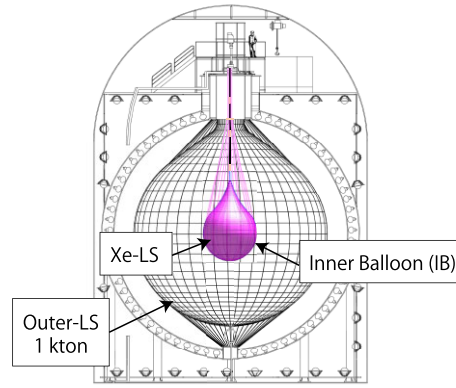


Fig. 3. Schematic diagram of the KamLAND-Zen detector.

loss. Although it is not easy to increase the source mass as in calorimeter experiments, external source experiments provide excellent angular correlation and individual energy measurements of the two emitted electrons. In the future, this feature will be important for distinguishing between the different underlying mechanisms of $0\nu\beta\beta$.

In this article, I focus on the results of the $0\nu\beta\beta$ search in KamLAND-Zen, which most stringently limits the Majorana neutrino mass.

4. KamLAND-Zen

The KamLAND detector is a 1 kton liquid scintillator detector located 1000 m underground at the Kamioka mine in Japan, as illustrated in Fig. 3. Scintillation light is viewed by 1325 17-inch and 554 20-inch photomultiplier tubes (PMTs) mounted on an 18-m-diameter spherical stainless-steel tank. Taking advantage of its low-background feature, KamLAND has achieved the world's first observation of reactor antineutrino oscillations [14,15] and the detection of geo-neutrinos [16,17]. This low-background feature also allows for a high-sensitivity $0\nu\beta\beta$ search with the addition of several detector components. Liquid scintillator (LS) can be loaded with $\beta\beta$ isotopes of ^{136}Xe , which is best suited for use in KamLAND for the following reasons: (i) Isotopic enrichment of ^{136}Xe gas by centrifugation is possible. (ii) Xenon gas is chemically stable and dissolves about 3 wt% in the LS. (iii) Slow $2\nu\beta\beta$ decay requires modest energy resolution. (iv) The well-known 2.614 MeV γ from ^{208}Tl is not a serious background for ^{136}Xe $0\nu\beta\beta$ (the Q -value is 2.458 MeV) because the coincident β/γ from ^{208}Tl are detected in homogeneous active detectors. Aiming at the $0\nu\beta\beta$ search in the IO region, 800 kg of enriched xenon (91% ^{136}Xe) was prepared. The xenon was purified by distillation and refined with a heated zirconium getter. The water-dropped shape balloon was constructed by fixing 24 gores with a specially developed heat welding method. The folded balloon was sunk into the KamLAND detector through a narrow hole at the top, and inflated with the LS without xenon. Finally, the LS was replaced with the xenon-loaded LS (Xe-LS), as shown in Fig. 4.

The first data-taking at KamLAND-Zen began in 2011 [18]. The $\beta\beta$ decay source, 320 kg of xenon, was installed into a 3.08-m-diameter balloon. The first search showed event excess in the $0\nu\beta\beta$ signal region, which was identified as the background from ^{110m}Ag decays, based on the energy spectrum and event rate variation [19]. The $^{134}\text{Cs}/^{137}\text{Cs}$ ratio revealed that the Xe-LS is contaminated by the Fukushima fallout. Since the sensitivity of the $0\nu\beta\beta$ search was limited by the background, ^{110m}Ag was removed by Xe-LS purification [20]. First, xenon was extracted

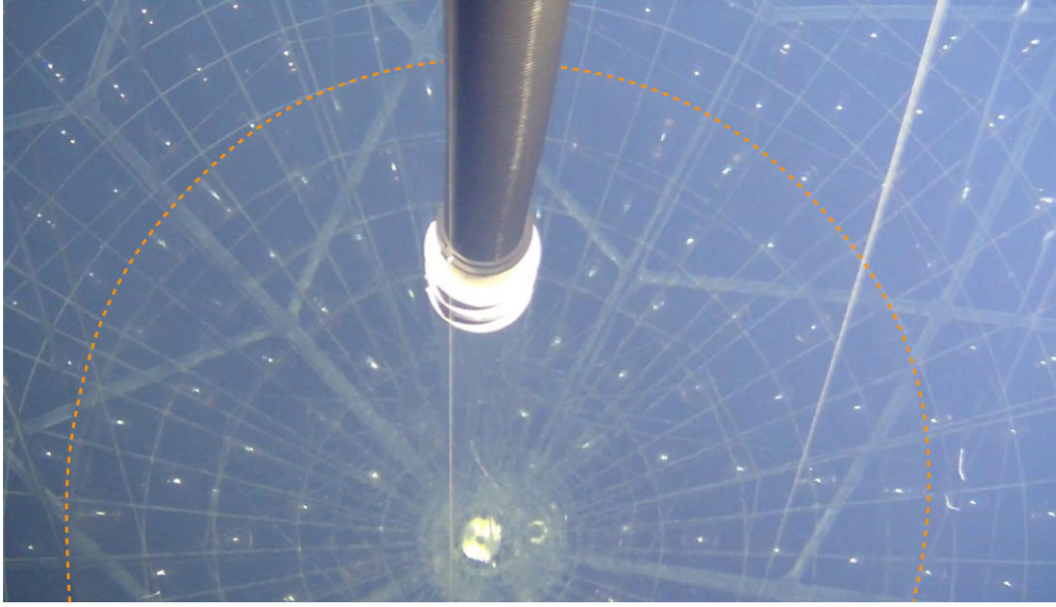


Fig. 4. Inside view of the KamLAND-Zen detector. The balloon was filled with the xenon-loaded liquid scintillator (Xe-LS). The dashed line shows the outline of the balloon shape.

from the detector by LS circulation to confirm the remaining ^{110m}Ag , and then the estimated background rate was cross-checked by on/off (Xe-LS/Xe-depleted-LS) measurement. After the purification, 380 kg of xenon was installed in 2013. The $0\nu\beta\beta$ search was continued until 2015, then most of the quasidegenerate neutrino mass region was surveyed [21]. To reach the IO region, the KamLAND-Zen detector was upgraded to a larger Xe-LS volume (3.80-m-diameter balloon) containing 745 kg xenon, corresponding to a twofold increase, and data-taking began in 2019. This search has provided a first test of the Majorana nature of neutrinos in the IO region.

I briefly discuss the latest result of the $0\nu\beta\beta$ search, which combines all KamLAND-Zen data up to May 2021 [22]. The $2\nu\beta\beta$ decays are observed with the highest statistics, and the measured $2\nu\beta\beta$ decay half-life of ^{136}Xe is $T_{1/2}^{2\nu} = 2.23 \pm 0.03(\text{stat}) \pm 0.07(\text{syst}) \times 10^{21} \text{ yr}$ [23]. Due to the limited energy resolution, the resolution tail of the $2\nu\beta\beta$ events is one of the major background sources, as discussed below. The data with 745 kg xenon contribute most significantly to the $0\nu\beta\beta$ search sensitivity. In this phase, the background due to radioactive impurities is dominated by ^{238}U and ^{232}Th daughter decays in the Xe-LS and balloon, and ^{110m}Ag decays are absent. ^{214}Bi decays (^{238}U daughter) are effectively removed by delayed coincidence tagging in the LS and are almost negligible; however, the untagged contributions on the balloon introduce backgrounds in the outer region within the Xe-LS volume. In this phase, this contamination was reduced to approximately one-tenth of that in the previous phase [21] because the balloon was fabricated more cleanly. In the inner region, the background due to cosmogenic spallation products is the largest: cosmic-ray muons penetrating the Xe-LS can cause energetic reactions that produce spatially uniform isotopes from carbon and xenon spallation. The products with lifetimes greater than $O(100)\text{s}$, denoted as “long-lived products”, are attributed to the decay of heavy isotopes produced by xenon spallation. Xenon spallation can be characterized by detecting multiple neutrons. Based on a likelihood-based discriminant, $(42.0 \pm 8.8)\%$ of xenon spallation backgrounds are removed. The total live time is 523.4 d.

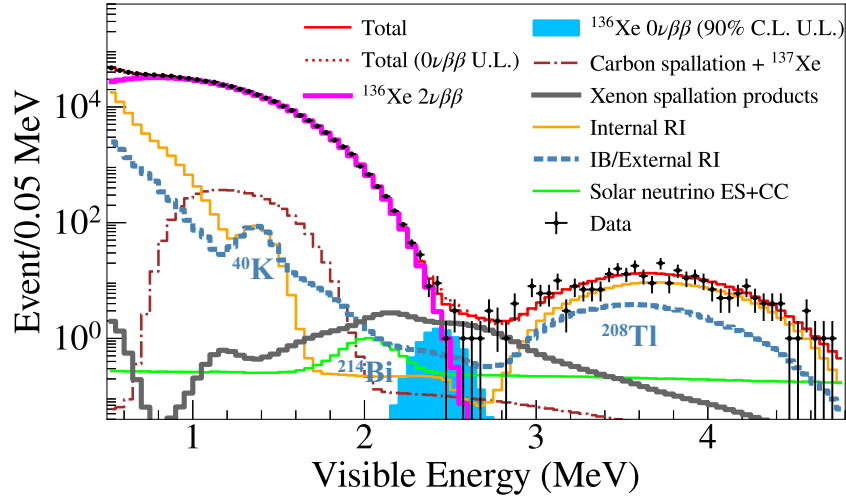


Fig. 5. Energy spectra of selected $\beta\beta$ candidates (singles data) within a 1.57-m-radius spherical volume drawn together with the best-fitting backgrounds, the $2\nu\beta\beta$ decay spectrum, and the 90% C.L. upper limit for $0\nu\beta\beta$ decay. The primary backgrounds in the $0\nu\beta\beta$ region are $2\nu\beta\beta$, xenon spallation, and radioactive impurities (RI) mainly at the inner balloon (IB).

Figure 5 shows the energy spectrum observed in KamLAND-Zen after removing the xenon spallation backgrounds. While there was no event excess from the $0\nu\beta\beta$ signal, the spectral fit provides the most stringent limit on the ^{136}Xe $0\nu\beta\beta$ decay half-life of $T_{1/2}^{0\nu} > 2.3 \times 10^{26}$ yr at 90% C.L., combining the analysis of the previous data-sets. The corresponding 90% C.L. upper limit on the effective Majorana neutrino mass $\langle m_{\beta\beta} \rangle$ is in the range 36–156 meV, based on Eq. (3) using the phase-space factor calculation from Refs. [24,25] and commonly used nuclear matrix element estimates [26–38], assuming the axial coupling constant $g_A \simeq 1.27$. Figure 2 shows the prediction of $\langle m_{\beta\beta} \rangle$ from neutrino oscillation parameters [4,39] as a function of the lightest neutrino mass m_{lightest} , together with the experimental limits from the $0\nu\beta\beta$ decay searches in ^{136}Xe [22], ^{76}Ge [7], and ^{130}Te [9]. The widths of the IO and NO bands reflect the uncertainties mainly due to the Majorana CP phases, which cause cancellations of neutrino masses in $\langle m_{\beta\beta} \rangle$. If no cancellations occur, the predicted values of $\langle m_{\beta\beta} \rangle$ with $m_{\text{lightest}} = 0$ are 4 meV and 48 meV for NO and IO, respectively. The search in ^{136}Xe begins to test the IO band below 50 meV, and realizes the partial exclusion of some theoretical models [40–42] that estimate $\langle m_{\beta\beta} \rangle$ based on predictions of the CP phases.

The sensitivity of the $0\nu\beta\beta$ search in KamLAND-Zen is limited by the primary background from xenon spallation products and $2\nu\beta\beta$ decay, as shown in Fig. 5. In the current detector, multiple neutrons just after xenon spallation by muons are not fully detected due to a deadtime in the electronics. In order to improve the removal efficiency of the xenon spallation background, state-of-the-art electronics that maximizes neutron detection efficiency is planned to be installed. Removal of xenon spallation background by particle identification is also a practical method. Most of the xenon spallation backgrounds are due to the radioactive decays, which emit not only e^- or e^+ (β decay) but also coincident de-excitation γ or e^+e^- pair annihilation γ . Thus, background events from xenon spallation products have multisite energy deposits in the Xe-LS spreading over $O(10\text{ cm})$ distances due to γ -ray diffusion, while the $0\nu\beta\beta$ events are localized in smaller $< 1\text{ cm}$ distances. Such dispersion of scintillation location can be statistically evaluated by using the photon hit time of the PMTs. To remove the xenon spallation

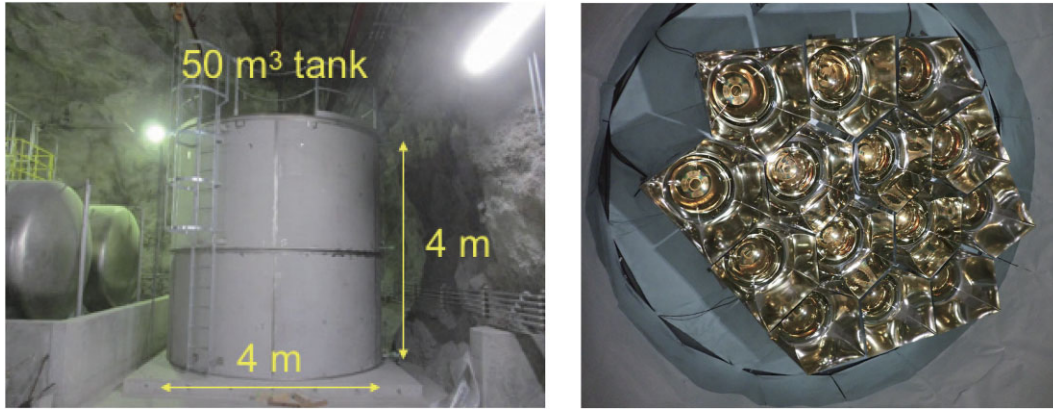


Fig. 6. KamLAND2-Zen prototype detector: (left) 50 m³ tank and (right) high quantum efficiency (HQE) PMTs with light collective mirrors in the tank.

backgrounds, an integrated spatiotemporal deep neural network, referred to as KamNet [43], was developed in KamLAND-Zen. A simulation study using KamNet showed the ability to improve the $0\nu\beta\beta$ search sensitivity by the background removal.

In the future, the KamLAND detector is planned to be upgraded to improve the $0\nu\beta\beta$ search sensitivity, denoted as KamLAND2-Zen. The discrimination between $0\nu\beta\beta$ and $2\nu\beta\beta$ can be improved by the upgraded detector with better energy resolution. The energy resolution (σ) improves from 4.0% to $<2.5\%$ at the Q -value of ^{136}Xe $0\nu\beta\beta$ decay. This will be achieved by employing light collective mirrors ($>1.8\times$ light yield), new brighter LS ($1.4\times$ light yield), and high quantum efficiency (HQE) PMTs ($1.9\times$ light yield). To maximize light collection, new polygonal mirrors, which do not have the dead space of conventional circular mirrors, were newly developed. To demonstrate this high detector performance, the KamLAND2-Zen prototype, which consists of a 50 m³ stainless tank, 14 HQE PMTs and light collective mirrors, new brighter LS, and new state-of-the-art electronics, has been constructed at the Kamioka mine (Fig. 6). The data-taking in the prototype will begin soon. In addition, a scintillation balloon film made of polyethylene naphthalate (PEN) has also been developed to remove the backgrounds from the balloon film by an α -tagging method. Also, research is underway to effectively reduce γ -emission backgrounds using a scintillation imaging system to identify multisite energy deposits. To reduce the solar neutrino background, a double concentration of ^{136}Xe loading into the LS with pressurized xenon is also being investigated. The expected sensitivity in KamLAND2-Zen is $\langle m_{\beta\beta} \rangle \sim 20$ meV, allowing a nearly full survey of the IO region, and the possibility of finding the $0\nu\beta\beta$ signal will be greatly enhanced.

5. Conclusion

The Majorana neutrino, proposed more than 80 years ago, is still a major research topic in particle physics. In this article, I have described the current status and prospects of the $0\nu\beta\beta$ decay search. In particle physics and cosmology, the Majorana neutrino is the key to explaining the light neutrino masses and the matter dominance of the universe. In addition, $0\nu\beta\beta$ decay allows us to investigate the absolute neutrino mass, complementing searches in beta decay measurements and cosmological observations. Reflecting the importance of the $0\nu\beta\beta$ search, a number of experimental projects using modern technology are planned. The result in KamLAND-Zen, using an ultra-low-background detector and an unprecedented 745 kg of enriched xenon, has

provided the most stringent limit on the Majorana neutrino mass, and the high sensitivity search is continuing. Although there was no experimental evidence of $0\nu\beta\beta$ decay, much progress has been made in the improved searches. Given the rapid progress in recent years, it would not be surprising if $0\nu\beta\beta$ decay is found in the near future.

Acknowledgements

The author gratefully acknowledges the members of the KamLAND-Zen Collaboration, providing information about their research activities and recent progress.

Funding

Open Access funding: SCOAP³.

References

- [1] M. Goeppert-Mayer, Phys. Rev. **48**, 512 (1935).
- [2] W. H. Furry, Phys. Rev. **56**, 1184 (1939).
- [3] E. L. Fireman, Phys. Rev. **74**, 1238 (1948).
- [4] I. Esteban, M.C. Gonzalez-Garcia, M. Maltoni, T. Schwetz, and A. Zhou (2020), Nufit 5.0: Three-neutrino fit based on data available at <http://www.nu-fit.org>.
- [5] M. Aker et al. [KATRIN Collaboration], Nat. Phys. **18**, 160 (2022).
- [6] N. Aghanim et al. [Planck Collaboration], Astron. Astrophys. **641**, A6 (2020).
- [7] M. Agostini et al. [GERDA Collaboration], Phys. Rev. Lett. **125**, 252502 (2020).
- [8] N. Abgrall et al. [LEGEND Collaboration], [\[arXiv:2107.11462](https://arxiv.org/abs/2107.11462) [physics.ins-det]] [[Search inSPIRE](#)].
- [9] D. Q. Adams et al. [CUORE Collaboration], Nature **604**, 53 (2022).
- [10] K. Alfonso et al. [CUPID Collaboration], J. Low Temp. Phys. (2022), <https://doi.org/10.1007/s10909-022-02909-3>.
- [11] G. Anton et al. [EXO Collaboration], Phys. Rev. Lett. **123**, 161802 (2019).
- [12] J. B. Albert et al. [nEXO Collaboration], Phys. Rev. C **97**, 065503 (2018).
- [13] M. J. Dolinski, A. W. P. Poon, and W. Rodejohann, Ann. Rev. Nucl. Part. Sci. **69**, 219 (2019).
- [14] K. Eguchi et al. [KamLAND Collaboration], Phys. Rev. Lett. **90**, 021802 (2003).
- [15] S. Abe et al. [KamLAND Collaboration], Phys. Rev. Lett. **100**, 221803 (2008).
- [16] T. Araki et al. [KamLAND Collaboration], Nature **436**, 499 (2005).
- [17] A. Gando et al. [KamLAND Collaboration], Nat. Geosci. **4**, 647 (2011).
- [18] A. Gando et al. [KamLAND-Zen Collaboration], Phys. Rev. C **85**, 045504 (2012).
- [19] A. Gando et al. [KamLAND-Zen Collaboration], Phys. Rev. Lett. **110**, 062502 (2013).
- [20] I. Shimizu and M. Chen, Front. Phys. **7**, 33, (2019).
- [21] A. Gando et al. [KamLAND-Zen Collaboration], Phys. Rev. Lett. **117**, 082503 (2016).
- [22] S. Abe et al. [KamLAND-Zen Collaboration], Phys. Rev. Lett. **130**, 051801 (2023).
- [23] A. Gando et al. [KamLAND-Zen Collaboration], Phys. Rev. Lett. **122**, 192501 (2019).
- [24] J. Kotila and F. Iachello, Phys. Rev. C **85**, 034316 (2012).
- [25] S. Stoica and M. Mirea, Phys. Rev. C **88**, 037303 (2013); updated in [\[arXiv:1411.5506v3](https://arxiv.org/abs/1411.5506v3) [nucl-th]] [[Search inSPIRE](#)].
- [26] N. L. Vaquero, T. R. Rodríguez, and J. L. Egido, Phys. Rev. Lett. **111**, 142501 (2013).
- [27] J. M. Yao, L. S. Song, K. Hagino, P. Ring, and J. Meng, Phys. Rev. C **91**, 024316 (2015).
- [28] T. R. Rodríguez and G. Martínez-Pinedo, Phys. Rev. Lett. **105**, 252503 (2010).
- [29] F. F. Deppisch, L. Graf, F. Iachello, and J. Kotila, Phys. Rev. D **102**, 095016 (2020).
- [30] J. Barea, J. Kotila, and F. Iachello, Phys. Rev. C **91**, 034304 (2015).
- [31] L. Coraggio, A. Gargano, N. Itaco, R. Mancino, and F. Nowacki, Phys. Rev. C **101**, 044315 (2020).
- [32] A. Neacsu and M. Horoi, Phys. Rev. C **91**, 024309 (2015).
- [33] J. Menendez, A. Poves, E. Caurier, and F. Nowacki, Nucl. Phys. A **818**, 139 (2009).
- [34] J. Terasaki, Phys. Rev. C **102**, 044303 (2020).
- [35] J. Hyvärinen and J. Suhonen, Phys. Rev. C **91**, 024613 (2015).
- [36] F. Šimkovic, V. Rodin, A. Faessler, and P. Vogel, Phys. Rev. C **87**, 045501 (2013).
- [37] M. T. Mustonen and J. Engel, Phys. Rev. C **87**, 064302 (2013).

- [38] D.-L. Fang, A. Faessler, and F. Šimkovic, Phys. Rev. C **97**, 045503 (2018).
- [39] S. Dell’Oro, S. Marcocci, and F. Vissani, Phys. Rev. D **90**, 033005 (2014).
- [40] K. Harigaya, M. Ibe, and T. T. Yanagida, Phys. Rev. D **86**, 013002 (2012).
- [41] T. Asaka, Y. Heo, and T. Yoshida, Phys. Lett. B **811**, 135956 (2020).
- [42] K. Asai, Eur. Phys. J. C **80**, 76 (2020).
- [43] A. Li, Z. Fu, C. Grant, H. Ozaki, I. Shimizu, H. Song, A. Takeuchi, and L. A. Winslow, Phys. Rev. C **107**, 014323 (2023).